A model for predicting smoke back-layering length in tunnel fires with the combination of longitudinal ventilation and point extraction ventilation in the roof

Junheng Wang[a,b,c], Jianping Yuan[a,b], Zheng Fang[a,b], Zhi Tang[a,b,*], Peng Qian[c], Jianqiao Ye[a,c]

[a] School of Civil Engineering, Wuhan University, Wuhan 430072, China

[b] Engineering Research Centre of Urban Disasters Prevention and Fire Rescue Technology of Hubei Province, Wuhan 430072, China

[c] Department of Engineering, Lancaster University, Lancaster LA1 4YR, U.K.

Abstract: An analytical model is developed for quantifying the fire smoke back-layering length in a tunnel with a combination of longitudinal ventilation and point extraction ventilation in the roof. The distance of smoke vent to fire source is incorporated as well as mass flow rate during the whole smoke flow process according to the mass conservation principle. The model input quantities are the heat release rate of the fire source, the longitudinal velocity, the exhaust velocity, the width and the height of the tunnel, the distance of the smoke vent to the fire source and the area of the smoke vent. The quality of the model predictions is illustrated for a range of experimental conditions. After that, extensive model predictions on the back-layering length are presented to show its trends by varying the velocity of the longitudinal ventilation, the exhaust velocity and the position of the smoke vent in the roof. Discussions are given at last. It is highlighted that shortening the distance between the smoke vent and the fire source benefits shortening the back-layering length, and this phenomenon is more pronounced for higher exhaust velocity.

*Corresponding author. Tel.:+86 027 68772312

E-mail address: zhi.tang@whu.edu.cn（Zhi Tang）.

Key words: Tunnel fire; Longitudinal ventilation; Point extraction; Back-layering length

Nomenclature

A	area of the smoke vent, m
A_t	cross-sectional area of the tunnel, m^2
B	tunnel width, m
C	coefficient constant
c_p	specific heat capacity, $kJ/(kg \cdot K)$
d	distance from smoke vent to fire source, m
D	contact length, m
D'	characteristic length
Fr	Froude number
Fr_m	modified Froude number
g	gravitational acceleration, m/s^2
h	smoke layer height, m
H	tunnel height, m
H_d	height from fire source to tunnel ceiling, m
K	longitudinal decay coefficient of the ceiling excess temperature
K'	modified longitudinal decay coefficient of the ceiling excess temperature
K_1	longitudinal decay coefficient of the ceiling excess temperature downstream the smoke vent
l	back-layering length, m
l'	the second part of back-layering length, m
l^*	dimensionless back-layering length
l^{**}	modified dimensionless back-layering length
$\dot{m}$	plume mass flow rate, $kg \cdot s$
$\dot{Q}_c$	convective heat release rate, kW
$\dot{Q}$	heat release rate, kW
$\dot{Q}^*$	dimensionless heat release rate
$\dot{Q}^{**}$	modified dimensionless heat release rate
r	radius of the fire source, m
Ri'	modified Richardson number
T	temperature, K
V	velocity, m/s
V^*	dimensionless longitudinal velocity
V^{**}	modified dimensionless longitudinal velocity
V'	longitudinal velocity induced by both the longitudinal ventilation and the point extraction, m/s
V_a	longitudinal velocity induced by the longitudinal ventilation, m/s
V_c	critical velocity, m/s
w^*	characteristic plume velocity, m/s
x	coordinate at the virtual x-axis, m
x_0	coordinate of the positon of the maximum excess ceiling temperature, m

Greek symbols

α	heat transfer coefficient
γ	experiments coefficient
ε	experiments coefficient
ρ	density, kg/m^3
θ	flame angle, °
Δ	excess over the initial value
δ	proportional coefficient

Subscript

0	initial value
a	ambient
ex	exhaust
in	induced
max	max value
r	residual
s	stagnation
up	upstream

1. Introduction

In the last few decades, tunnel fires have caused a lot of damage to properties and casualties [1-3], and the fire smoke is the leading reason. The danger of the smoke in tunnel fire not only results from the visibility obscuring effect but also from its toxicity. The ventilation systems are then applied in tunnels to deal with the fire smoke and the longitudinal ventilation system is a common one. The principle of the longitudinal ventilation is to blow the fire smoke to the downstream of the fire source so that the upstream side would be clear for evacuation and rescue. However, sometimes the longitudinal air flow would be smaller than the critical velocity due to the poor ventilation capability, large fire scale or the “throttling effect”. As a result, the smoke would spread upstream of the fire source and then the back-layering (upstream traveling of the smoke in the direction opposite to the ventilation) occurs. Apparently, the smoke back-layering would danger the evacuees and the rescuers upstream of the fire and lead to an increase in number of casualties in tunnel fires. So it is significant to study and quantify the back-layering length in the case of the tunnel fire.

Many scholars have developed models for quantifying the back-layering length, but most of them were developed in the contests of the tunnels with the longitudinal ventilations. Because of destroying the stratification of the smoke downstream of the fire source, the limitation in the use of the longitudinal ventilation system is apparent. The longitudinal ventilation is preferably applied to non-congested tunnels where there are normally no people downstream of the fire source. As for the urban tunnels designed for queues, it is a challenge to only adopt a sole longitudinal ventilation system. To take this challenge, the longitudinal ventilation is often designed together with the extraction ventilation in Chinese urban tunnels (e.g. Wuhan Yangtze River tunnel and Nanjing Yangtze River tunnel). When a fire occurs, the smoke vent closed to the fire source would open to assist in exhausting the fire smoke. It is no doubt that the point extraction ventilation in the roof would interact with the longitudinal ventilation system to affect the formation of the smoke back-layering. Present paper will focus on this phenomenon and build a model to quantify the length of the back-layering under the combined effect of the longitudinal ventilation and the point extraction ventilation in the roof.

The structure of this paper is as follows. A review of the models for quantifying smoke back-layering flow length is presented firstly. Then, the phenomenon described by the model is introduced before the introduction of the phenomenon described by the model. Next, the accuracy of the model for predicting the back-layering length is illustrated by means of the experimental data and a third party model. Afterwards, the influences of the longitudinal velocity, the exhaust velocity and the distance of the smoke vent from the fire source on the back-layering length are discussed, and some conclusions are made at last.

2. Literature review

In the previous research, many models [4-8] have been developed to predict the length of back-layering. However, most of them are aim to serve for the purely longitudinal ventilated tunnels, and a few studies consider the contexts of the combination of the longitudinal ventilation and the point extraction ventilation in the roof.

In 1958, a theory of describing the back-layering length was proposed by Thomas[8] in 1958. In [8], the dimensionless back-layering length, l^*, was correlated with a modified Froude number, $Fr_m = \frac{gH\Delta T}{{V_a}^2(T_a+\Delta T)}$. The proposed relation was expressed as follows:

$$l^* = \frac{l}{H} \propto \frac{gFr_m}{\rho_a c_p V_a \Delta T A_t} \quad (1)$$

where g is the gravitational acceleration, H is the tunnel height, ρ_a is ambient air density, c_p is the specific heat capacity of air, l is the back-layering length, V_a is the longitudinal velocity, A_t is the cross-sectional area of the tunnel, T_a is the ambient temperature. ΔT is the temperature excess over ambient.

In 1991, Vantelon et al. [5] defined a modified Richardson number, $Ri' = \frac{g\dot{Q}_0}{\rho_a T_a c_p {V_a}^3 H}$, and proposed that the dimensionless back-layering length varied as 0.3 power of Ri', given as:

$$l^* \propto Ri'^{0.3} \tag{2}$$

where $\dot{Q}_0$ is the heat release rate of the fire source.

In 2001, based on the experiments performed in a model tunnel of Paris metro, Deberteix et al. [7] correlated the back-layering length with the Richardson number, $Ri = \frac{gD'\Delta T}{{V_a}^2 T_a}$, to proposed the equation as follows:

$$l^* = 7.5\left(Ri^{1/3} - 1\right) \tag{3}$$

where D' is a characteristic length.

In 2010, Li and Ingason et al. [6] performed small-scale experiments and correlated the dimensionless smoke back-layering length to the dimensionless heat release rate of the fire source and the dimensionless longitudinal velocity. The correlation shows as follows:

$$l^* = \begin{cases} 18.5\ln(0.81{\dot{Q}^*}^{1/3}/V^*),\ \dot{Q}^* \le 0.15 \\ 18.5\ln(0.43/V^*),\ \dot{Q}^* > 0.15 \end{cases} \tag{4}$$

where

$l^* = \frac{l}{H}$

(5)

$V^* = \frac{V_a}{\sqrt{gH}}$

(6)

$\dot{Q}^* = \frac{\dot{Q}_0}{\rho_a c_p T_a g^{1/2} H^{5/2}}$.

(7)

Considering the driving force of the fire smoke, the upstream smoke flow should stop at the place where the static pressure balances to the dynamic pressure caused by the longitudinal ventilation. Based on this theory, Chow et al. [4] studied the back-layering length in a tilted tunnel with longitudinal ventilation, and calculated the back-layering length with the ceiling temperature. The expression gives as:

$$l = -\frac{1}{K} ln\left[\frac{V_a{}^2}{gh_0}\frac{1}{\gamma\left(\dot{Q}^{*2/3}/Fr^{1/3}\right)^{\varepsilon}}\right] \tag{8}$$

where γ, ε are coefficients obtained by the experiments [9], K is the longitudinal decay coefficient of the ceiling excess temperature, h_0 is the initial smoke layer height, Fr is the Froude number.

Apart from the models introduced above, Hu et al. [10] developed models of quantifying the back-layering length for the purely longitudinal ventilated tunnels. Along with the same research methodologies as descried previously, some scholars tried to study the effect of the point extraction by the smoke vent on the back-layering. Vauquelin et al. [11, 12] experimentally investigated the smoke flow profiles in a scaled tunnel with a point extraction system and defined the "confinement velocity" at which the smoke layering length would be confined to be certain value by the induced wind. Ingason and Li [13] conducted small-scale experiments to study the single point and two-point extraction system combining with the longitudinal ventilation or the natural ventilation handling with the HGV fires. Chen et al. [14] established a mathematical model to predict the two-directional smoke back-layering length with a combination of the point extraction and the longitudinal ventilation. In that work, a smoke vent was set just above the fire source. The correlations were expressed as:

$$l^{**} = \begin{cases} 18.5\ln(0.81\dot{Q}^{**\,1/3}/V^{**}),\ \dot{Q}^{**} \le 0.15 \\ 18.5\ln(0.43/V^{**}),\ \dot{Q}^{**} > 0.15 \end{cases} \tag{9}$$

With

$$\dot{Q}^{**} = \frac{\dot{Q}_0 - c_p \rho_{ex} V_{ex} A \Delta T_{max}}{\rho_\text{a} c_p T_\text{a} g^{1/2} H^{5/2}} \qquad (10)$$

$$l^{**} = \frac{l}{H} \qquad (11)$$

and

$$V^{**} = \frac{V_a + \rho_{ex} V_{ex} A / 2BH\rho_0}{\sqrt{gH}} \qquad \text{for the upstream} \qquad (12)$$

$$V^{**} = \frac{\rho_{ex} V_{ex} A / 2BH\rho_a - V_a}{\sqrt{gH}} \qquad (V_a < \rho_{ex} V_{ex} A / 2BH\rho_a) \qquad \text{for the downstream} \qquad (13)$$

where ρ_{ex} is the density of exhaust smoke, V_{ex} is the exhaust velocity, A is the area of smoke vent, ΔT_{max} is the maximum temperature excess the ambient, B is the tunnel width.

However, the fire does not always occur just below the smoke vent. Chen et al. [15] further carried out experiments with the smoke vent at different downstream distance from the fire source. The previously established mathematical model (Eq.9) [14] was also able to predict l^{**} in the contexts of the smoke vent locating downstream of the fire source by giving:

$$\dot{Q}^{**} = \frac{\dot{Q}_0 - c_p \rho_{ex} V_{ex} A \Delta T_{max} e^{-Kd}}{\rho_a c_p T_a g^{1/2} H^{5/2}} \qquad (14)$$

where d is the distance from smoke vent to the fire source.

Models in both [14] and [15] describe the smoke vent located just above the fire source and at the downstream side respectively. In fact, the smoke vent upstream of the fire source would be operated as well. As a consequence, the smoke vent upstream of the fire source might directly exhaust the smoke from the smoke back-layering, so that the back-layering length would be different from the situation that the smoke vent is operating at the downstream side [15]. And it had been confirmed by the experiments conducted by Tang et al. [16]. In their experimental configuration [16], the smoke vent was set upstream of the fire source compared to the experiments conducted by Chen et al. [15]. The experiment results observed by Tang et al. [16] highlighted that the smoke back-layering length in their experiments was shorter than that from experiments conducted by Chen et al. [15]. Based on the experimental data, they proposed a modified longitudinal decay coefficient of the ceiling excess temperature (K') in the model of Chen et al. [15] (Eq.14):

$$K' = \left(\frac{V_c}{V_c - V_a}\right)^{0.3} \times \frac{\alpha D}{c_p\left(0.071\dot{Q}_0^{\,1/3} H_d^{\,5/3} - \dot{m}_{ex}\right)} \quad (15)$$

where V_c is the critical velocity, α is the heat transfer coefficient, H_d is the height from the fire source to tunnel ceiling, $\dot{m}_{ex}$ is the mass flow rate of the exhaust smoke .

Yao et al.[17] have done similar experimental work, focusing on the smoke back-layering flow length in the longitudinal ventilated tunnel with vertical shaft by the natural ventilation on the upstream side of the fire source. They also proposed a modified prediction model derived from the model of Li et al. [6].

As already reviewed, there are many literatures focusing on the smoke back-layering length, but the relevant research on the smoke back-layering in the contexts of the combination of the longitudinal ventilation and the point extraction ventilation was not many found. The existing models for quantifying these phenomenon [14-16] were all based on the model proposed by Li et al. [6], deriving from the dimensionless correlation between the smoke back-layering length and the longitudinal velocity. The effect of the point extraction ventilation on the back-layering was considered by introducing a reduced heat release rate of the fire source, $\dot{Q}^{**}$, from the point view of the heat conservation. However, the mass conservation during the whole spread process of the back-layering was not incorporated into the existing models yet. As it is obviously that the mass flow rate is an important parameter for the formation of the back-layering, particularly for the mass flow rate changing at the smoke vent position, a model would be developed in this research to take this challenge. More specifically, the smoke back-layering is divided into two regions by the smoke vent, and the whole process of smoke spreading through the smoke vent is considered in the model development based on mass and energy conservation principles.

3. Model development

Fig. 1 shows the sketch of the phenomenon described in the model. There is a fire occurring in a tunnel, and a smoke back-layering is formed upstream of the fire source. The smoke back-layering is suppressed by the combined effect of the longitudinal ventilation and the point extraction ventilation in the roof upstream of the fire source, because the fire smoke would be blown to the downstream by the longitudinal air flow and be extracted out of the tunnel by the smoke vent in the roof. A virtual x-axis is introduced and the origin is set just above the fire source. Fig. 1 also displays the distance between the smoke vent and the fire source, d, and the stagnation point where is the smoke back-layering stopping propagating.

Indeed, the process of the smoke spreading in the tunnel as shown in Fig.1, is similar to the smoke propagation in the tunnel with the longitudinal ventilation, apart from that partial smoke being removed by the smoke vent which is immerged in the smoke back-layering. Consequently, it is logical that the model for quantifying the back-layering length in Fig. 1 can be developed in a similar way to the models only taking the longitudinal ventilation system into account. According to Fig.1, the back-layering length can be divided into two parts: (1) the smoke flow length between the smoke vent and the origin (the fire source); (2) the smoke flow length between the smoke vent and the stagnation point.

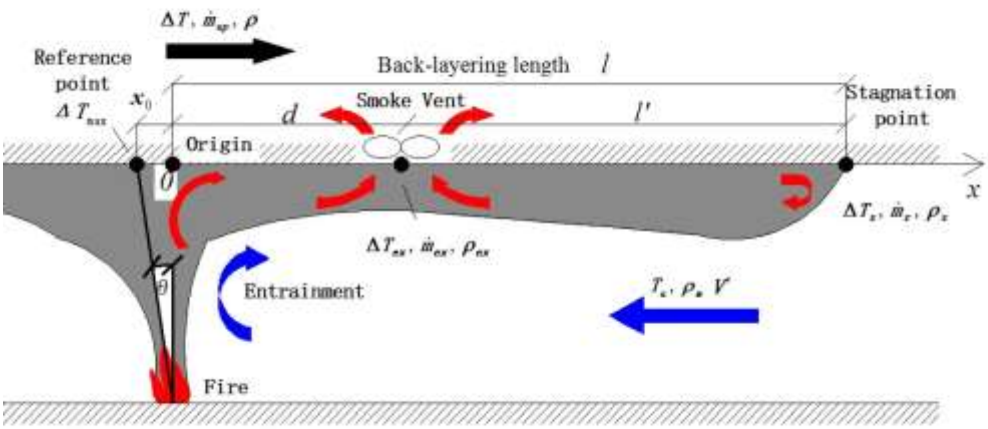

Fig.1 Schematic diagram of the fire smoke spreading with the point extraction ventilation and the longitudinal ventilation

The first part of the back-layering length equals to the distance between the smoke vent and the fire source, *d*.

The second part of the back-layering length is the length of the smoke flow that begins from the position of the smoke vent. Thus the second part of the smoke back-layering length can be determined by the smoke characteristics (e.g. the smoke mass flow rate and the temperature) at the position of the smoke vent and the longitudinal velocity induced by both of the longitudinal ventilation and the point extraction ventilation in the second part region. The similar methodology of calculating the back-layering length under the longitudinal ventilation [4, 10] can be referred to the calculations in this region. Therefore, it is key to quantify the smoke characteristics (e.g. the smoke mass flow rate and the temperature) at the location of the smoke vent where is the boundary condition of the second part of the back-layering length. The details of the equations for calculating the temperature and the mass flow rate of the smoke layer will be presented next, following the propagation process as shown below.

Generally, the movement of the fire smoke in the tunnel is subdivided into several regions [18-23]. The process of the smoke spreading is divided into 3 regions in this study, as shown in Fig.2. Regions I and III are the symmetrical ceiling jet region and the one-dimensional spreading region, respectively, while region II is the radial spreading and transition region.

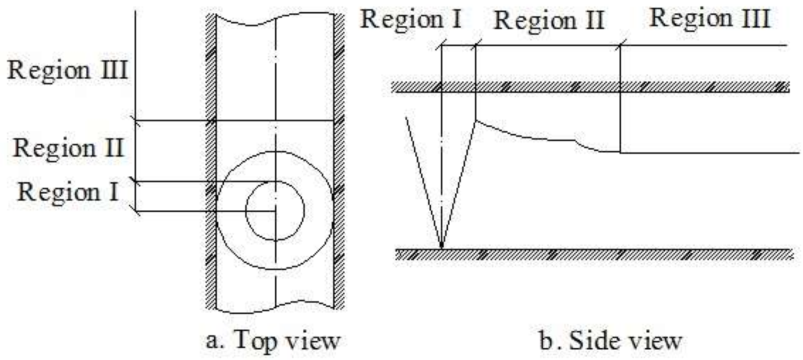

Fig.2 Schematic diagram of smoke spreading in tunnels

In Region I, the fire plume rises up from the fire source and propagates horizontally after impinging the ceiling. Massive air is entrained from the surrounding atmosphere, because of the vertical motion of the buoyant smoke. Thus, the smoke volume increases greatly due to the entrainment. According to [24], the mass flow rate of the upwards fire plume is given as:

$$\dot{m}_0 = 0.071\dot{Q}_c^{\,1/3} H^{5/3} \tag{16}$$

When a longitudinal ventilation system operates, the flame of the fire source would be deflected, as shown in Fig.3. There is more fresh air entrained into the tilted fire plume than before. Consequently, the mass flow rate of the smoke must be modified. Li et al.[25, 26] proposed a model to predict the mass flow rate of the tilted fire plume under the effect of the longitudinal ventilation,

$$\dot{m}_0 = \begin{cases} 0.3735\dot{Q}_c^{1/3} H_d^{5/3} V^*, & V^* > 0.19 \\ 0.071\dot{Q}_c^{1/3} H_d^{5/3}, & V^* \leq 0.19 \end{cases} \tag{17}$$

with $$V^* = \frac{V_a}{w^*} \tag{18}$$

$$w^* = \left(\frac{\dot{Q}_c g}{r\rho_0 c_p T_0}\right)^{1/3} \quad (19)$$

where w^* is the characteristic plume velocity, V_a is the longitudinal velocity, V^* is the dimensionless longitudinal velocity.

Fig.3 Flame deflection

It is noteworthy that the mass flow rate of the upstream spreading smoke, $\dot{m}_{up}$, depends on the value of the longitudinal velocity. As such, $\dot{m}_{up}$ is expressed as:

$$\dot{m}_{up} = \delta \dot{m}_0 \quad (20)$$

where δ is proportional coefficient, range from 0 to 0.5. Due to lack of experimental data, previous studies [17] always take $\delta = 0.5$ for calculations.

The maximum excess ceiling temperature over ambient can be expressed as Eq.21 [26]:

$$\Delta T_{max} = \begin{cases} \frac{\dot{Q}_0}{V_a r^{1/3} {H_d}^{5/3}}, V^* > 0.19 \\ 17.5 \frac{\dot{Q}_0^{2/3}}{{H_d}^{5/3}}, V^* \leq 0.19 \end{cases} \quad (21)$$

where r is radius of the fire source.

Since the fire plume tilts to the downstream side of the fire source, the position of the maximum excess ceiling temperature would be shifted to the downstream of the fire source, and its coordinate is written as x_0, as shown in Fig.1. The displacement is correlated to the tilt angle of the flame. The tilt angle is expressed as follow based on the theory proposed by Thomas et al.[27]:

$$cos\theta = \begin{cases} 1, & V^* \leq 0.19 \\ (5.26V^*)^{-1/2}, & V^* > 0.19 \end{cases} \quad (22)$$

Hence, the coordinate of the reference point (the position of the maximum excess ceiling temperature) can be written as:

$$x_0 = -H_d tan\theta \quad (23)$$

Region II is a transit region. After impinging on the ceiling, the smoke turns to radial spreading from the reference point until the smoke reaches the side walls of the tunnel. After that, the one-dimensional smoke spreading in the tunnel longitudinal direction occurs, and the one-dimensional smoke spreading region is formed. Compared with the one-dimensional smoke spreading region, the range of the transit region is relatively short, so the friction between the smoke and the ceiling, the entrainment and the heat loss to the ceiling in the transit region are all neglected, following the previous studies [18, 19, 21-23, 28]. It is then reasonable to assume that the heat and the mass remain conservative in the transit region.

Region III is a one-dimensional spreading region, and the movement of the smoke can be easily described by the conservation equations.

Thus, the smoke excess temperature decaying along the tunnel from the reference point can be predicted and a simple model were deduced by Hu [28], given as:

$$\frac{\Delta T}{\Delta T_{\max}} = e^{-K(\mathrm{x}-x_0)} \quad (24)$$

where x is the coordinate, x_0 is the coordinate of the position of the maximum excess ceiling temperature, ΔT is the smoke excess temperature over ambient in the roof at x, $\Delta T_{\max}$ is the smoke maximum excess temperature over ambient in the roof (at x_0);

K is the ceiling temperature decay coefficient:

$$K = \frac{\alpha D}{c_p \dot{m}_{up}} \tag{25}$$

with D is the length that smoke contact to the tunnel in cross section, it reads

$$D = 2h_0 + B \tag{26}$$

The entrainment is neglected at this region [18, 19, 28], so the height of ceiling jet is assumed unchanged. The initial height of the smoke layer in the one-dimension region relates only to the distance from the surface of the fire source to the ceiling and the width of the tunnel [19, 21, 22], given as:

$$h_0 = CH\left(\frac{B}{2H}\right)^{1/3} \tag{27}$$

where C is coefficient constant, ranging from 0.2128 to 0.2483.

Further, the heat transfer coefficient,α, can be also approximately considered as a constant in the calculation [18]. The same conclusion was also made from the full-scale and model experiments performed by Hu et al. and Chen et al. [15, 28-30]. Therefore, based on the Eq.24 introduced above, the temperature distribution of the first part of the smoke back-layering, the smoke layer between fire source and the smoke vent, can be calculated. Inserting Eq.25 into Eq.24, the smoke excess temperature at the positon of the smoke vent, ΔT_{ex}, can be calculated by Eq.28:

$$\Delta T_{ex} = \Delta T_{max} e^{-\frac{\alpha D}{c_p \dot{m}_{up}}(d-x_0)} \tag{28}$$

It is known that some of the smoke would be removed by the smoke vent, while the residual spreads over the smoke vent and continue propagating upstream, as shown in Fig.1. Ignoring the entrainment at Region II and Region III, and based on the mass conservation principle, the mass flow rate of the smoke spreading over the smoke vent, $\dot{m}_r$, equals to the initial mass flow rate of the smoke spreading upstream, $\dot{m}_{up}$, subtracting the amount of the smoke extracted by the smoke vent, $\dot{m}_{ex}$, given as:

$$\dot{m}_r = \dot{m}_{up} - \dot{m}_{ex} \tag{29}$$

where $\dot{m}_{ex}$ can be written as:

$$\dot{m}_{ex} = \rho_{ex} V_{ex} A \tag{30}$$

It is assumed that the extraction system does not cause the "plug-holing", which makes the smoke spreading over the smoke vent (the second part of the back-layering) staying in one-dimensional spreading. Thus, the temperature still decreases exponentially with the tunnel length.

The back-layering should stop spreading upstream at the place where the static pressure balances to the dynamic pressure caused by both the longitudinal ventilation and the point extraction ventilation. The position of the smoke stagnation point under the longitudinal ventilation can be derived from excess temperature, ΔT_s , at the stagnation point as reported by Chow et.al [4]. The expression is given as:

$$\frac{\Delta T_S}{T_a} = \frac{V'^2}{g h_0} \tag{31}$$

It is noteworthy that h_0 is the height of the smoke layer;

V' is the modified longitudinal velocity induced by both of the longitudinal ventilation and the point extraction ventilation in the roof, given as:

$$V' = V_{in} + V_a \tag{32}$$

where V_a, V_{in} is the velocity induced by the longitudinal ventilation and the point extraction ventilation in the roof respectively. Furthermore, V_{in} can be obtained by

$$V_{in} = \frac{\dot{m}_{ex}}{2BH\rho_a} \quad (33)$$

As illustrated previously, Eq.24 still applies in this region, then Eq.24 converting to Eq.34:

$$\Delta T_s = \Delta T_{ex} e^{-K_1 l'} \quad (34)$$

where ΔT_{ex} is the excess smoke temperature at the smoke vent, which can be obtained by Eq.28;

K_1 is the ceiling temperature decay coefficient downstream the smoke vent;

$$K_1 = \frac{\alpha D}{c_p \dot{m}_r} \quad (35)$$

l' is the second part of the smoke back-layering length.

Substituting Eq.31 into Eq.34 yields

$$\Delta T_{ex} e^{-K_1 l'} = T_a \frac{V'^2}{g h_0} \quad (36)$$

Combining Eq.28 and Eq.36, it gets

$$\Delta T_{max} e^{-K(d-x_0)} e^{-K_1 l'} = T_a \frac{V'^2}{g h_0} \quad (37)$$

Thus, the second part of the back-layering length, l' , can be expressed as:

$$l' = -\frac{1}{K_1} ln\left(\frac{V'^2}{g h_0}\frac{T_a}{\Delta T_{max}}\right) - \frac{K}{K_1}(d - x_0) \quad (38)$$

Substituting Eq.17-23, 25-27, 29-30, 32-33, 35 into Eq.38, the second part of the smoke back-layering length can be analytically calculated.

Combining two components, the smoke back-layering length finally writes:

$$l = d + l' \quad (39)$$

4. Results and discussion

4.1 Comparison to experimental data

Since it is not available to conduct validation tests by ourselves in this study, experimental data of Tang et al., reported in ref. [16], would be used for model validation. First, the phenomena observed in the tests of Tang et al. [16] are the same as prescribed in the model. Furthermore, the values for modelling parameters were all measured or quantified in the tests of Tang et al. [16]. Therefore, experimental data of Tang et al. [16] are available for validating the present model.

The experiments in [16] were conducted in a reduced-scale (a scale of 1/6) model tunnel with dimensions of $72\ m$ (length) $\times\ 1.5\ m$ (width) $\times\ 1.3\ m$ (height) [14-16]. The fire source was located at the central of the tunnel. A circular smoke vent (diameter of $0.3\ m$) was settled at the middle of the tunnel ceiling. More specifically, it was installed 1 *m* upstream the fire source (*d*=1 *m*). A longitudinal ventilation system was also installed at the entrance of the tunnel model. The parameters, including the heat release rate of the fire source, the exhaust velocity and the longitudinal velocity, were variables in the tests. The smoke back-layering lengths were derived from the measured ceiling temperature distributions in the experiments. The thermocouples were arranged at an interval of $0.5\ m$.

Table.1 Summary of valid scenarios in the experiments [16]

Test No.	Heat release rate (*kW*)	Exhaust velocity (*m/s*)	Longitudinal velocity (*m/s*)
1~9	30	0.5, 1, 1.5, 2, 2.2	0.3, 0.5
10~18	40	0.5, 1, 1.5, 2, 2.2	0.3, 0.5
19~27	50	0.5, 1, 1.5, 2, 2.2	0.3, 0.5

Recall that the present model applies to one smoke vent immerged inside the smoke back-layering which implies that the back-layering length is longer than the distance from the smoke vent to the fire source d and no plug-holing occurs, as shown in Fig.1. Therefore, the available experimental data from [16] used for illustrating the accuracy of the model are the back-layering lengths longer than 1 m, as the smoke vent in the roof is located 1 m upstream the fire source in the experimental configuration [16]. Table 1 summarises the information of the experiments used for comparing.

Before illustrating the agreement that is obtained between predictions and experiments, there needs to quantifying the uncertainty in the measured output quantities (l) and input quantities ($\dot{Q}_0$, V_a, V_{ex}). The latter component attributes to the propagation of input parameter uncertainty respectively. As the thermocouples were arranged at an interval of $0.5\ m$ to quantify the smoke back-layering length, l, the uncertainty of the measurements of l is $\pm 0.5\ m$. Additionally, the heat release rate of the fire source was controlled by a gas flow meter with accuracy of $\pm 0.1\ m^3/h$ [14-16]. Thus, the relatively uncertainty in HRR measurement can be roughly calculated to be 8%. Both the longitudinal velocity and the pointed exhaust velocity were measured by a digital hot-wire anemometer. Due to lack of details of the hot-wire anemometer, the measurement uncertainties of the velocity are estimated as 3%, according to the work reported by F.E. Jørgensen [31].

Based on the uncertainty analysis above, comparisons of the predictions from the present model to experimental data of Tang et al. [16] are provided in Fig.5 The horizontal uncertainty bar represents uncertainty in the experiment measurement of the back-layering length while the vertical bar represents the propagation of input parameter uncertainty resulting from the uncertainty in the HRR, longitudinal velocity and exhaust velocity. The diagonal line with a slope of 1 is employed to evaluate the discrepancy between the model predictions and the experimental data. Clearly, all the results are concentrated along the line and a general satisfactory agreement is observed.

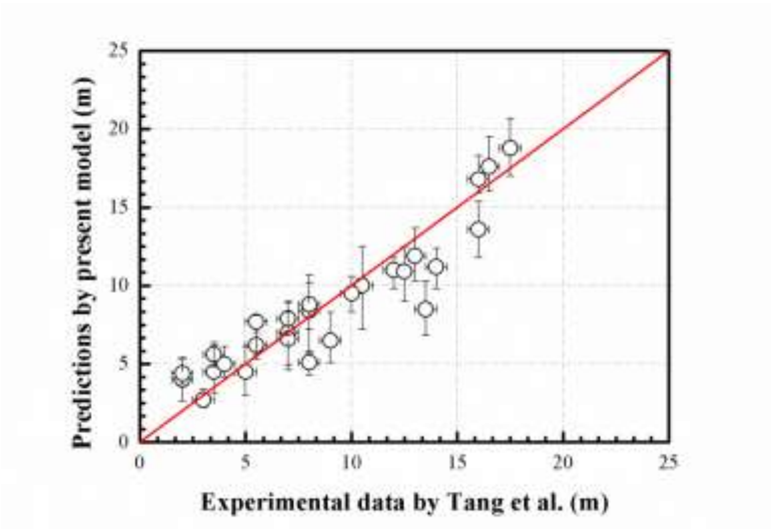

Fig.5 Comparison of the predictions with the experimental results in [16]

The horizontal uncertainty bar and vertical uncertainty bar represents uncertainty in the experiment measurement of the back-layering length and the propagation of input parameter uncertainty respectively.

4.2 Comparison to other model results

As described in the introduction section, the model of Tang et al. [16] is the only existing model for predicting the smoke back-layering for the conditions of the longitudinal ventilated tunnel with the smoke vent in the roof upstream the fire source. Although it is not a straightway to verify the present model by comparing to another model, it is still interesting to make this kind of comparisons in this section as the two models were developed by two different methodologies, as introduced previously.

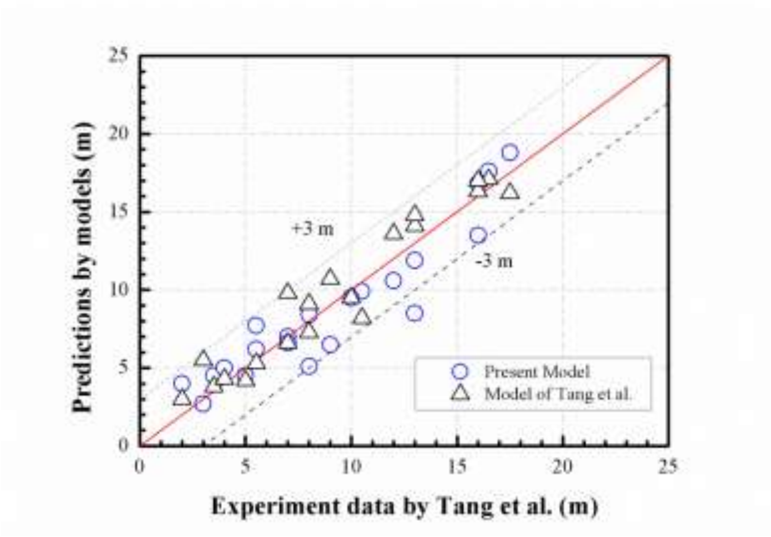

Fig.6 Comparison to the results calculated by the model of Tang et al.

The results calculated by the model of Tang et al. [16] and the present model are illustrated in Fig.6. The abscissa is the back-layering length measured in the experiments, while its ordinate is the results predicted by the two models. The circles represent the predictions of the present model, and the triangles represent the predictions of the other model. Fig. 6 shows that the predicted plots are closed to the diagonal line with a slope of 1. Two dash lines are drawn with the offset of 3 *m* to display the deviation between the predictions of the models and the experimental data. It is clear that the predictions of both models are almost located between these two dash lines, which means the deviations of both predictions are less than 3 *m*. So the plots from both models are closed to each other.

Although Figure 6 shows the two models give similar predictions, a discussion is necessary on the difference of two models. As illustrated previously, the two models were developed by two different approaches. The model of Tang et al. incorporates the effect of the point extraction ventilation on the length of back-layering via a reduced heat release rate of the fire source, $\dot{Q}^{**}$, from the point view of the heat conservation. As a result, the model of Tang et al. for quantifying the length of back-layering, as shown in Eq. 9, is only associated with $\dot{Q}^{**}$

and $\dot{V}^{**}$. The detailed mass and heat transfer along the smoke back-layering was not taken into account. The present model, by contrast, incorporates much more of fire smoke spread details, ceiling jets, and mass flow rate calculations than does the existing model. For example, the smoke back-layering described in the present model is divided by the smoke vent location into two regions, each of which is resolved by including the mechanism from the mass and heat conservations principles. As a consequence, one benefit of the present model is able to explicitly explore the impact of the smoke vent location on the back-layering length (see section 4.4). Additionally, the present model is ambitious and convenient to be further developed to a universal model to predict the back-layering length in the longitudinally ventilated tunnel with multiple smoke vents activated.

4.3 Prediction of the back-layering length under different ventilation condition

Experimental data in [16] show that the smoke back-layering length is dramatically influenced by the longitudinal ventilation velocity as well as the velocity of the point extraction ventilation in the roof. In this section, more results are calculated by the present model to supplement the experimental data to discuss the influences of the two kinds of ventilations on the smoke back-layering lengths.

4.3.1 Different longitudinal ventilation velocity

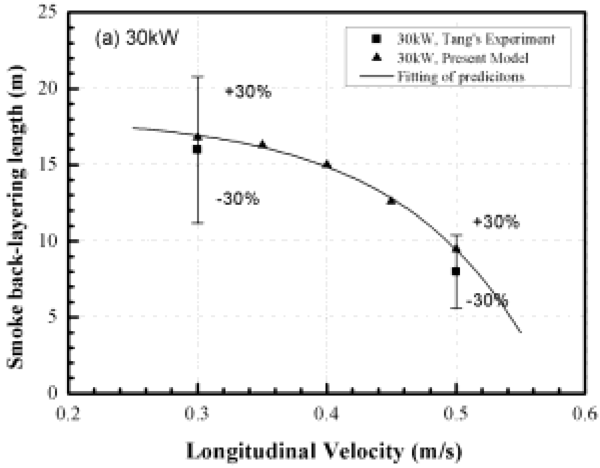
(a) 30kW
30kW, Tang's Experiment
30kW, Present Model
Fitting of predicitons
+30%
-30%
+30%
-30%
Smoke back-layering length (m)
Longitudinal Velocity (m/s)
0
5
10
15
20
25
0.2
0.3
0.4
0.5
0.6

(a)

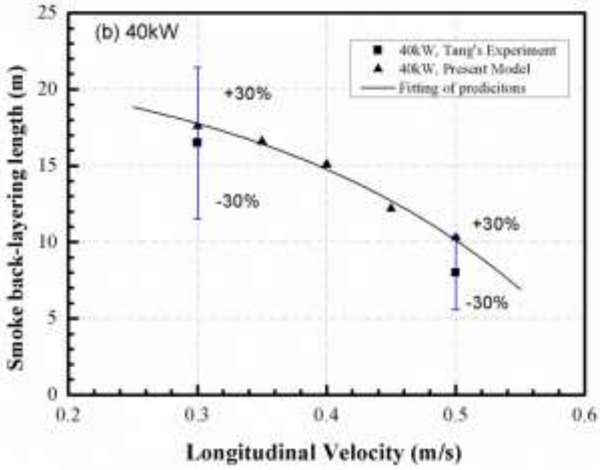
(b) 40kW
40kW, Tang's Experiment
40kW, Present Model
Fitting of predicitons
+30%
-30%
+30%
-30%
Smoke back-layering length (m)
Longitudinal Velocity (m/s)
0
5
10
15
20
25
0.2
0.3
0.4
0.5
0.6

(b)

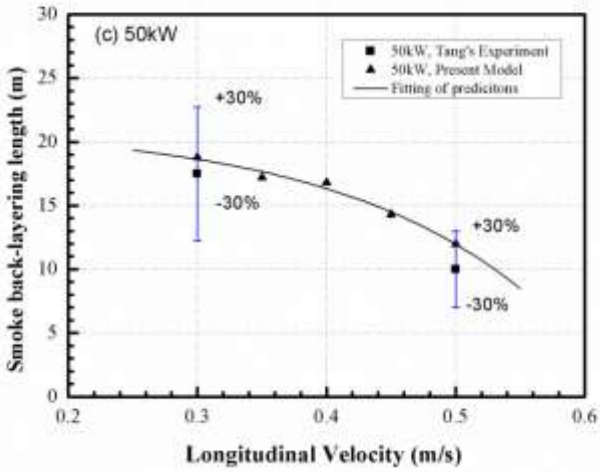
(c) 50kW
50kW, Tang's Experiment
50kW, Present Model
Fitting of predicitons
+30%
-30%
+30%
-30%
Smoke back-layering length (m)
Longitudinal Velocity (m/s)
0
5
10
15
20
25
30
0.2
0.3
0.4
0.5
0.6

(c)

Fig.7 The smoke back-layering lengths varying with different longitudinal velocities ($V_{ex} = 1.0\, m/s$) (a): HRR=30 kW; (b): HRR=40 kW; (c); HRR=50 kW.

The predictions of the smoke back-layering length with different longitudinal velocities are compared to the experimental results measured in [16], as shown in Fig.7. The exhaust velocity is set at $1.0\, m/s$ in all tests. Fig.7 (a), (b) and (c) represents 30 kW, 40 kW and 50 kW heat release rate respectively. The curves displayed in Fig.7 are drawn by fittings of the predictions, while the rectangles present the experimental results.

The prediction curves in Fig.7 just well captured the similar tendency of the smoke back-layering length varying with the longitudinal velocity as observed in the experiments. The prediction error is less than 30%. It is logical that the prediction of the fire smoke back-layering length gets shorter as the longitudinal velocity becomes larger. Indeed, the increase of the dynamics pressure with the longitudinal velocity can suppress the fire smoke spreading upstream.

Fig. 7 also shows the good predictions of the smoke back-layering lengths for different HRRs. When the heat release rate grows, the fire smoke back-layering length becomes larger. Indeed, the increase of the smoke buoyancy momentum with HRR would increase the back-layering length, which has been well explained by Eq. 21 and Eq. 38.

4.3.2 Different exhaust velocity through the smoke vent in the roof

In order to show the impact of the ceiling smoke exhaust velocity on the smoke back-layering length, Fig. 8 is drawn to show the variations of the predictions of the back-layering length with different exhaust velocities. The experimental results are also presented in Fig. 8 for the purpose of comparison. The longitudinal velocity is $0.3\, m/s$ for all cases. All the three heat release rates in the experiments (*30 kW*, *40 kW* and *50 kW*) are considered. The exhaust velocity increases from 0.5 m/s to 2.2 m/s, referring to the exhaust velocity range in the experiments. The curves in the Fig.8 are determined by fittings of the predictions, while the plots present the experiments results.

Clearly, the experimental results show that increase of exhaust velocity would reduce the smoke back-layering length, e.g. keeping the fire heat release rate of 30 kW and the longitudinal velocity of 0.3 m/s constant, the back-layering length decreases from 17 m to 3.5 m, when the exhaust velocity grows from 0.5 m/s to 2.2 m/s. Less smoke spread to the upstream side in larger exhaust velocity due to more smoke removed by the extraction system, so that the residual smoke can be more easily suppressed by the longitudinal air flow. In addition, Fig. 7 also illustrates the accuracy of the present model in predicting the smoke back-layering lengths for different HRR and exhaust velocity.

It notes that the lines fitting by the predictions are straight line while it is not the case for the experimental plots, resulting in moderate gaps between the predictions and the experimental results (but still less than 35%). The reason is that the effect of the point extraction ventilation on the fire plume, which is confirmed in [16] due to the short distance between the fire source and the smoke vent, is not considered in the present model at this research stage. Further work about the interaction between the fire plume and the extraction system are needed.

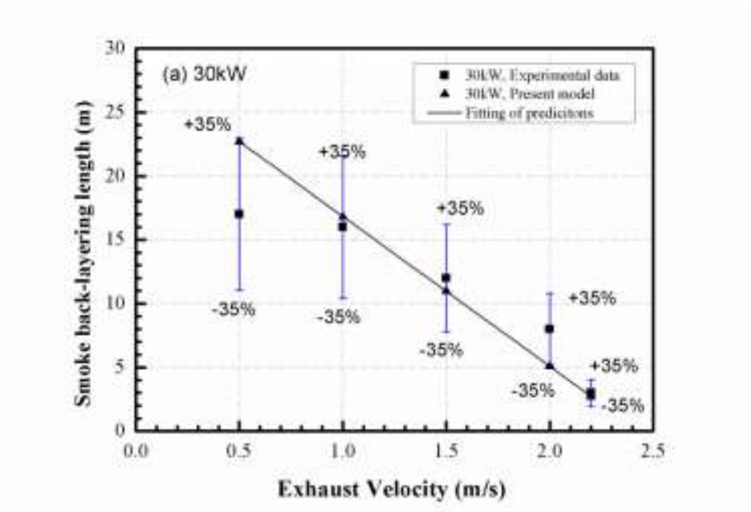

(a)

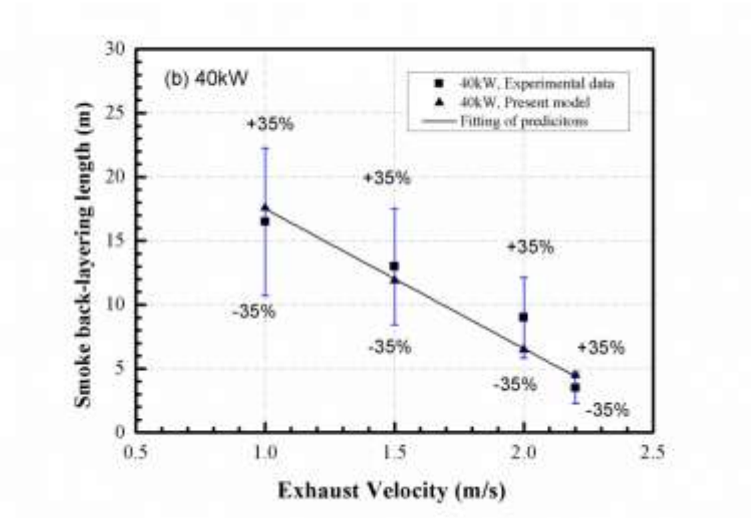

(b)

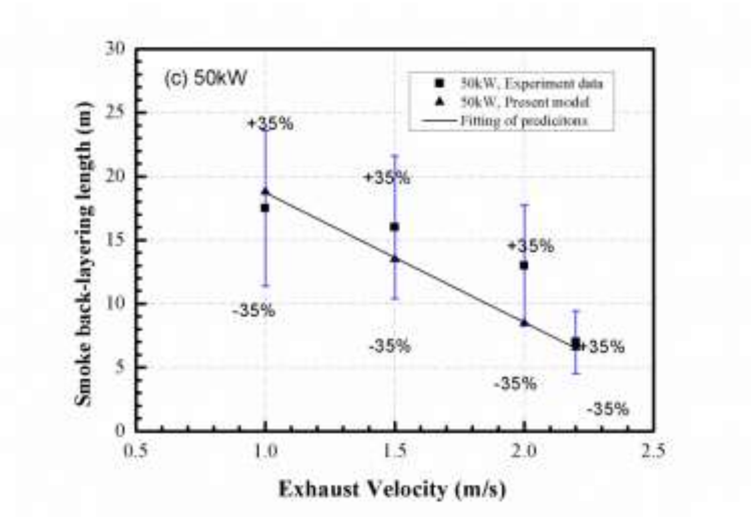

(c)

Fig.8 The smoke back-layering lengths variation with different exhaust velocities

$(V_a = 0.3\, m/s)$

4.4 Prediction of the back-layering length for different smoke vent location

Because the temperature of the removed smoke is related to the positon of the smoke vent away from the fire source, *d* should have apparent impact on the smoke back-layering length in the tunnel fire. It is significant to use the present model to show and discuss the influence of the distance d on the back-layering length. Changing the upstream position of the smoke vent, the smoke back-layering lengths are calculated by the present model. One heat release rates ($40\ kW$) and two longitudinal velocities ($0.3\ m/s$, $0.5\ m/s$) and a range of exhaust velocities are considered. The results are shown in Fig.9.

In Fig.9, every single curve represents a certain value of the back-layering length with different V_{ex} and d. The percentage for each curve as shown in Fig. 9, named as "reduction percentage" here, is one minus the ratio of the back-layering length under both of the longitudinal ventilation and the point extraction ventilation to that only under the longitudinal ventilation.

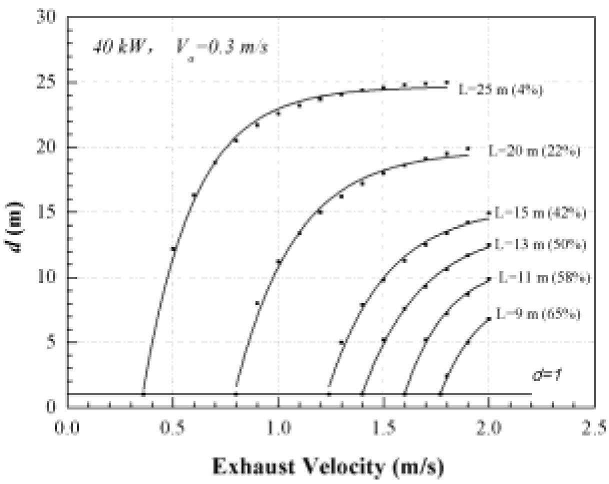

(a)

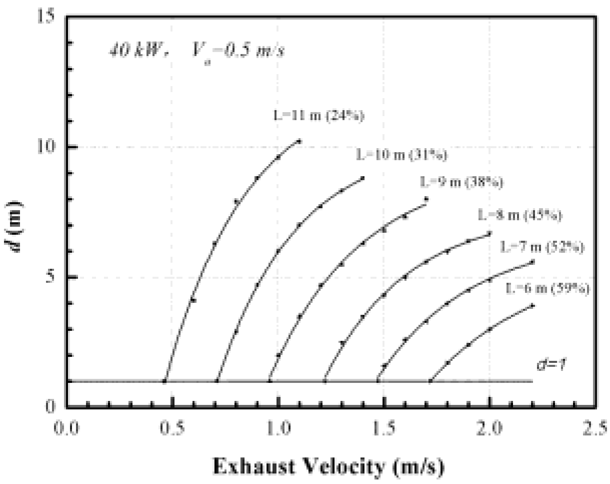

(b)

Fig.9 Predictions of the smoke back-layering lengths varying with different smoke vent position

(a) $V_a = 0.3\ m/s$ (b) $V_a = 0.5\ m/s$

Fig.9(a) shows the curves under the condition of $V_a = 0.3\ m/s$, presenting the values of the back-layering length range from $9\ m$ to $25\ m$. Despite of the difference in the coordinates and scales, the curves are similar to each other in tendency. It is clear to see that the back-layering length decrease as shortening the distance d and raising the exhaust velocity V_{ex}. It is not surprise to see this tendency because the smoke vent closer to the fire source with a larger exhaust velocity could exhaust larger amount of the smoke with higher temperature out of the tunnel, then resulting in reducing the buoyancy force of the back-layering. Particularly, when the distance d is larger than $15\ m$, the maximum reduction percentage of the back-layering length is less than 42% in this phenomenon, no matter how large the exhaust velocity is. With the decrease of d, the maximum reduction percentage would increase as well. For example, the maximum reduction percentage of the back-layering length would increase to 65% when $d = 7\ m$. It should also be highlighted that the distance d plays a more important role in reducing the back-layering length when the exhaust velocity is large. For example, when the exhaust velocity is smaller than 0.8 m/s, the reduction percentage of the back-layering length is ranged from 0% to 22% (0% happens when d is larger than the back-layering length, and 22% happens when $d = 0\ m$); When the exhaust velocity is larger than 1.75 m/s, the reduction percentage of the back-layering length is ranged from 0% to 65% (0% happens when *d* is larger than the back-layering length, and 65% happens when $d = 0\ m$)).

Fig.9 (a) also appears the correlations between the exhaust velocity and the back-layering length. For the curves of $l = 15\ m$, $l = 13\ m$, $l = 11\ m$, and $l = 9\ m$, the distances between adjacent curves almost equals to each other. Introducing a straight line of $d = 1\ m$, there are several points of intersection with these curves, representing the exhaust velocities for each back-layering length when $d = 1\ m$. It is interesting to note that the back-layering length linearly increase with the exhaust velocity, corresponding to the conclusions in section 3.3.2.

Fig.9(b) illustrates the curves of then back-layering lengths when the longitudinal velocity increase to 0.5 m/s. The same tendencies, as described above, are also observed here. However, compared to the curves with 0.3 m/s longitudinal velocity, as shown in Fig. 9(a), the *d* corresponding to a certain maximum reduction percentage in these phenomena is much smaller. For instance, $d = 15\ m$ in the tests with 0.3 *m/s* longitudinal velocity corresponding to 42% maximum reduction percentage, whereas about $d = 8\ m$ in the tests with 0.5 *m/s* longitudinal velocity corresponding to the same maximum reduction percentage. As discussed above, keeping other conditions constant, a smaller distance from the smoke vent to the fire source is expected to obtain a certain maximum reduction percentage as the longitudinal velocity increases.

5. Conclusions

In the paper at hand, an analytical model has been developed for quantifying the fire smoke back-layering length in tunnel with a combination of the longitudinal ventilation and the point extraction ventilation in the roof from first principles. Contrast to the existing models, a different approach has been applied in the model development. More importantly, the mass flow rate during the whole spread process of back-layering is cooperated in the present model. The model can be solved analytically with the input quantities (the heat release rate of fire source, the longitudinal velocity, the exhaust velocity, the width and height of the tunnel, the distance of the smoke vent to the fire source and the area of the smoke vent).

The accuracy of the model as presented has been illustrated by means of an experimental data set [16]. A comparison between of the present model and the model of Tang et al. [16] has also been made to see the comparability of the two models. Generally, satisfactory agreements have been obtained.

Extensive model predictions on the back-layering length, varying the velocity of the longitudinal ventilation, the exhaust velocity and the position of the smoke vent in the roof, have been done to illustrate its trends. The prediction of the back-layering length gets shorter as the longitudinal velocity or the exhaust velocity becomes larger, which is consistent with these phenomena in reality. It is interesting to note that the prediction of the back-layering length linearly increases with the decrease of the exhaust velocity, although the limited number of points in the tests at hand show more or less nonlinear tread.

Another important phenomenon discussed is that shortening the distance between the smoke vent and the fire source benefits shortening the back-layering length. The reduction of the back-layering length is more pronounced for higher exhaust velocity. It is also highlighted that a smaller distance from the smoke vent to the fire source is expected to obtain a certain maximum reduction percentage as the longitudinal velocity increases.

Since the analytical model at this research stage is simple, it is important to recall its limitations in order to avoid improper use. The model is only valid for the phenomenon that one smoke vent set upstream of the fire source combined with the longitudinal ventilation, as described in Fig. 1. Furthermore, the plug-holing phenomenon happening at the smoke vent is not in the application scope of the present model. Additionally, due to the interactions between the fire plume and the smoke vent was not considered in the present model, some error would be expected as the smoke vent near the fire source. In the future, based on the present model, more comprehensive model would be studied and developed by considering more smoke vents operated in the tunnel fire, the plug-holing phenomenon as well as the interactions between the fire plume and the smoke vent in the model.

Acknowledgements

This work is jointly supported by Natural Science Funds of China [Grant No. 51576144 and No. 51508426] and China Scholarship Council [Grant No.201506270067].

Reference

[1]. A.Hacck, *Fire Protection in Traffic Tunnels General Aspects and Results of the EUREKA Project.* Tunnelling and Underground Space Technology, 1998. **13**(4): p. 5.
[2]. F. Vuilleumier, A.W., B. Crausaz, *Safety aspects of railway and road tunnel example of the lotschberg railway tunnel and mont-blanc road tunnel.* Tunnelling and Underground Space Technology, 2002. **17**.
[3]. Leitner, A., *The fire catastrophe in the Tauern Tunnel-experience and conclusions for the Austrian guidelines.* Tunnelling and Underground Space Technology, 2001. **16**: p. 217-223.
[4]. Chow, W.K., et al., *Smoke movement in tilted tunnel fires with longitudinal ventilation.* Fire Safety Journal, 2015. **75**: p. 14-22.
[5]. J.P.Vantelon, et al. *Investigation of fire-induced smoke movement in tunnels and stations: an application to the Paris Metro*. in *Proceedings of the Third International Symposium on Fire Safety Science*. 1991. Edinburgh,UK: Elsevier.

[6]. Li, Y.Z., B. Lei, and H. Ingason, *Study of critical velocity and backlayering length in longitudinally ventilated tunnel fires.* Fire Safety Journal, 2010. **45**(6-8): p. 361-370.

[7]. P.Deberteix, D.Gabay, and D.Blay. *Experimental study of fire-induced smoke propagation in a tunnel in the presence of longitudinal ventilation*. in *Proceedings of the International Conference on Tunnel Fires and Escape from Tunnels*. 2001. Washington.

[8]. P.H.Thomas, *The movement of buoyant fluid against a stream and venting of underground fires*, in *Fire Research Note*. 1958, Fire Research Station: Watford, UK.

[9]. Kurioka, H., et al., *Fire properties in near field of square fire source with longitudinal ventilation in tunnels.* Fire Safety Journal, 2003. **38**(4): p. 319-340.

[10]. Hu, L.H., R. Huo, and W.K. Chow, *Studies on buoyancy-driven back-layering flow in tunnel fires.* Experimental Thermal and Fluid Science, 2008. **32**(8): p. 1468-1483.

[11]. O. Vauquelin, O.M., *Smoke extraction experiments in case of fire in a tunnel.* Fire Safety Journal, 2002. **37**: p. 9.

[12]. O. Vauquelin, D.T., *Definition and experimental evaluation of the smoke "confinement velocity" in tunnel fires.* Fire Safety Journal, 2005. **40**(4): p. 320-330.

[13]. Ingason, H. and L. Ying Zhen, *Model scale tunnel fire tests with point extraction ventilation.* Journal of Fire Protection Engineering, 2011. **21**(1): p. 5-36.

[14]. Chen, L.F., et al., *Studies on buoyancy driven two-directional smoke flow layering length with combination of point extraction and longitudinal ventilation in tunnel fires.* Fire Safety Journal, 2013. **59**: p. 94-101.

[15]. Chen, L.F., et al., *Thermal buoyant smoke back-layering flow length in a longitudinal ventilated tunnel with ceiling extraction at difference distance from heat source.* Applied Thermal Engineering, 2015. **78**: p. 129-135.

[16]. Tang, F., et al., *Thermal smoke back-layering flow length with ceiling extraction at upstream side of fire source in a longitudinal ventilated tunnel.* Applied Thermal Engineering, 2016. **106**: p. 125-130.

[17]. Yao, Y., et al., *Smoke back-layering flow length in longitudinal ventilated tunnel fires with vertical shaft in the upstream.* Applied Thermal Engineering, 2016. **107**: p. 738-746.

[18]. J.P.Kunsch, *Critical velocity and range of a fire-gas plume in a ventilated tunnel.* Atmospheric Environment, 1999. **33**: p. 13-24.

[19]. J.P.Kunsch, *Simple model for control of fire gases in a ventilated tunnel.* Fire Safety Journal, 2002. **37**: p. 67-81.

[20]. Delichatsios, M.A., *The flow of fire gases under a beamed ceiling.* Combustion and Flame, 1981. **43**: p. 1-10.

[21]. Oka, Y., H. Oka, and O. Imazeki, *Ceiling-jet thickness and vertical distribution along flat-ceilinged horizontal tunnel with natural ventilation.* Tunnelling and Underground Space Technology, 2016. **53**: p. 68-77.

[22]. Oka, Y. and H. Oka, *Velocity and temperature attenuation of a ceiling-jet along a horizontal tunnel with a flat ceiling and natural ventilation.* Tunnelling and Underground Space Technology, 2016. **56**: p. 79-89.

[23]. Li, S., et al., *Theoretical and experimental analysis of ceiling-jet flow in corridor fires.* Tunnelling and Underground Space Technology, 2011. **26**(6): p. 651-658.

[24]. Drysdale, D., *An Introduction to Fire Dynamics*. Third ed. 2011, Unitied Kingdom: John Wiley & Sons Ltd. 132-138.

[25]. Li, Y.Z. and H. Ingason, *The maximum ceiling gas temperature in a large tunnel fire.* Fire Safety Journal, 2012. **48**: p. 38-48.

[26]. Li, Y.Z., B. Lei, and H. Ingason, *The maximum temperature of buoyancy-driven smoke flow beneath the ceiling in tunnel fires.* Fire Safety Journal, 2011. **46**(4): p. 204-210.

[27]. Raj, P.K., et al., *Experiments Involving Pool and Vapor Fires from Spills of Liquefied Natural Gas on Water*. 1979: U.S. Coast Guard, Office of Research and Development.

[28]. Hu, L.H., et al., *Full-scale burning tests on studying smoke temperature and velocity along a corridor.* Tunnelling and Underground Space Technology, 2005. **20**(3): p. 223-229.
[29]. Hu, L.H., L.F. Chen, and W. Tang, *A global model on temperature profile of buoyant ceiling gas flow in a channel with combining mass and heat loss due to ceiling extraction and longitudinal forced air flow.* International Journal of Heat and Mass Transfer, 2014. **79**: p. 885-892.
[30]. Hu, L.H., et al., *A non-dimensional global correlation of maximum gas temperature beneath ceiling with different blockage–fire distance in a longitudinal ventilated tunnel.* Applied Thermal Engineering, 2013. **56**(1-2): p. 77-82.
[31]. Jørgensen, F.E., *How to Measure Turbulence with Hot- Wire Anemometers, a Practical Guide*. 2002, Denmark: Dantec Dynamics.